Elastic scattering and quasielastic transfer in the system $^{76,82}Se + ^{192,198}Pt$

F. L. H. Wolfs
Nuclear Structure Research Laboratory, University of Rochester, Rochester, New York 14627
and Argonne National Laboratory, Argonne, Illinois 60439

K. E. Rehm, W. C. Ma,* J. P. Schiffer, and T. F. Wang†
Argonne National Laboratory, Argonne, Illinois 60439
(Received 19 December 1991)

Elastic scattering and quasielastic transfer yields have been measured for $^{76,82}Se + ^{192,198}Pt$ using ^{76}Se and ^{82}Se beams with laboratory energies of 487.7 and 499.0 MeV, respectively. The variation of the one-neutron transfer yields as function of projectile and target mass can be understood on the basis of Q matching. Quasielastic transfer contributes at most 30% to the total reaction cross section with the remainder probably accounted for by deep-inelastic scattering.

PACS number(s): 25.70.Bc, 25.70.Hi

I. INTRODUCTION

The systematic study of the neutron-number dependence of the quasielastic transfer cross sections in the Ni+Sn system showed that their strength increases with increasing mass number of the target for the ^{58}Ni-induced reactions, while it is constant for the ^{64}Ni-induced reactions [1]. Although the behavior of the one-neutron transfer cross section can be understood from underlying nuclear structure effects, namely, the binding energy of the transferred particle and kinematic matching conditions during transfer [2], the dependence of the total quasielastic yield on neutron number of projectile and target is not yet understood. Both Ni and Sn have a closed proton shell ($Z=28$ and 50) and a possible influence of the shell closure on the total quasielastic cross section cannot be ruled out. In order to study the dependence of the quasielastic cross sections on neutron number for a system where shell effects should be minimal, we have measured elastic and quasielastic yields for $^{76,82}Se + ^{192,198}Pt$ at bombarding energies 35% above the Coulomb barrier, comparable to the Ni+Sn studies which were performed at about 30% above the barrier.

II. EXPERIMENTAL PROCEDURE AND DATA ANALYSIS

$^{76,82}Se$ beams from the Argonne Tandem Linac Accelerator System (ATLAS) were incident on targets of 80–140 $\mu g/cm^2$ $^{192,194,198}Pt$ evaporated onto a 10-$\mu g/cm^2$ ^{12}C backing. The enrichments of the targets used are 58.6, 95.1, and 95.3 % for ^{192}Pt, ^{194}Pt, and ^{198}Pt, respectively. The main contaminants in the ^{192}Pt target are ^{194}Pt (26.1%) and ^{195}Pt (11.0%). The measured yields on the ^{194}Pt target were used to extract the reaction yields for ^{192}Pt from the measured yields on the ^{192}Pt target. Based on the level of contamination and the observed variations of the yield as a function of neutron number, we believe that the error associated with this extraction is less than 10%.

The reaction products were momentum analyzed with an Enge split-pole spectrograph and detected in the focal plane with a position-sensitive ionization counter [3]. The position along the focal plane, the specific energy loss ΔE, and the total energy E were measured for each detected particle. In addition, the time of flight of the reaction products was measured with respect to the rf time structure of the beam, using a parallel-plate avalanche counter mounted in front of the ionization counter. The magnetic field in the spectrograph was chosen such that the 6–7 most abundant charge states were detected in the focal plane. The data were corrected for contributions from those charge states that were not detected in the focal plane for a given field setting, but these corrections were always less than 5%. Two silicon surface-barrier detectors, mounted at forward angles, were used to monitor the beam and target quality during the experiment, and for relative normalization between different runs. The absolute normalization was obtained using the elastic-scattering data at the forward-scattering angles, assuming that these yields are described by Rutherford scattering. The total error in this procedure is estimated to be 10%. The actual beam energy was measured using the time-of-flight energy measurement system of ATLAS [4] to be 487.7 and 499.0 MeV for the ^{76}Se and ^{82}Se beams, respectively. These energies were chosen such that the ^{76}Se-induced reactions were studied at about the same center-of-mass energies as the ^{82}Se-induced reactions.

From the position along the focal plane, the total energy, and the time of flight, the atomic charge of the reaction products can be calculated. For each atomic charge state, a mass spectrum was obtained using the measured position along the focal plane and the time of flight. Figure 1(a) shows an atomic charge-state distribution ob-

*Present address: Department of Physics and Astronomy, Vanderbilt University, Nashville, TN 37235.
†Present address: Lawrence Livermore National Laboratory, Livermore, CA 94550.

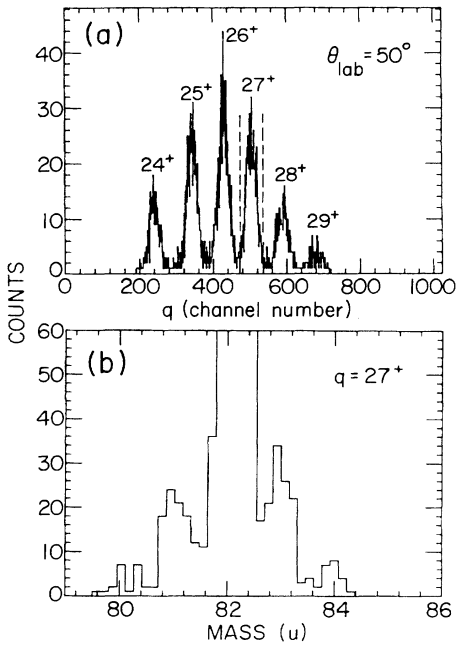

FIG. 1. (a) Atomic charge-state distribution and (b) mass spectrum gated on $q=27^+$, for ^{82}Se+^{198}Pt at $\theta_{lab}=50°$ and $E_{lab}=499.0$ MeV.

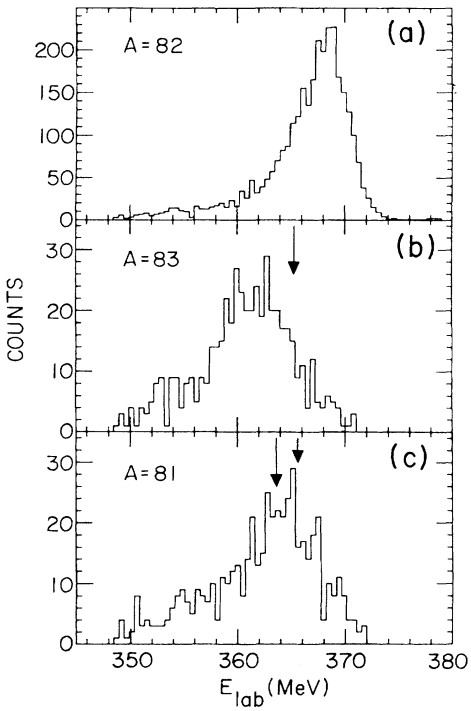

FIG. 2. Energy spectra for (a) elastic scattering, (b) one-nucleon pickup, and (c) one-nucleon stripping for ^{82}Se+^{198}Pt at $\theta_{lab}=50°$ and $E_{lab}=499.0$ MeV. The arrow in (b) indicates the laboratory energies corresponding to the ground-state Q values for one-neutron pickup. The arrows in (c) indicate the laboratory energies corresponding to the ground-state Q values for one-neutron stripping ($Q_{gg}=-3.70$ MeV) and one-proton stripping ($Q_{gg}=-5.87$ MeV).

tained for ^{82}Se+^{198}Pt at $\theta_{lab}=50°$. Figure 1(b) shows the mass spectrum obtained for the $q=27^+$ charge state [see gate in Fig. 1(a)]. The various transfer products can be clearly separated from the scattered beam particles.

The energy resolution obtained in the measurements was ≈ 4 MeV. This did not allow the separation of elastic scattering from inelastic excitation of low-lying states in projectile and target and the measured elastic-scattering cross sections will include these inelastic excitation yields. The total reaction cross sections, obtained from the measured "elastic-scattering" angular distributions, does not include the yields of inelastic excitation of low-lying states in projectile and target with a Q value more positive than -20 MeV. Likewise, in our analysis of quasielastic transfer reactions, we have only included those events with a Q value more positive than -20 MeV. Figure 2(a) shows an energy spectrum of scattered beam particles for ^{82}Se+^{198}Pt at $\theta_{lab}=50°$. Figures 2(b) and 2(c) show energy spectra of the reaction products for one-nucleon pickup and stripping reactions, respectively. The arrow in Fig. 2(b) indicates the laboratory energy corresponding to the ground-state Q value for one-neutron pickup. The arrows in Fig. 2(c) indicate the laboratory energies corresponding to the ground-state Q values for one-neutron and one-proton stripping reactions. The energy spectra of the transfer products are peaked around laboratory energies corresponding to small negative-Q values, indicating that the transfer occurs predominantly to low-lying states in the projectile-like and targetlike fragments.

The ΔE resolution achieved in this experiment was not sufficient to obtain an unambiguous Z identification of the reaction products. Figure 3 shows the Z spectra obtained from the E-ΔE spectra for reaction products with mass 81, 82, and 83 for ^{82}Se+^{198}Pt at $\theta_{lab}=50°$. The arrows in Fig. 3 indicate the calculated position of the $Z=33$ and 34 contributions. The one-nucleon pickup reactions are dominated by one-neutron pickup, while for the one-nucleon stripping reactions both proton and neutron stripping is important. The division of the total yield of the one-nucleon stripping reactions between neutron and proton stripping has large errors due to the poor Z resolution (see Fig. 3). Whenever possible, we will talk about the total one-nucleon stripping yields, whose errors are mainly determined by uncertainties in the statistics and in the absolute normalization. No attempts have been made to obtain Z identification for the products of two-nucleon stripping and pickup reactions.

III. EXPERIMENTAL RESULTS

A. Elastic scattering and the total reaction cross section

Figure 4 shows the measured elastic-scattering yields (including inelastic excitation with $|Q| \leq 20$ MeV) divided by the Rutherford cross section as function of the center-of-mass scattering angle for ^{76,82}Se+^{192,194,198}Pt. The solid curves in Fig. 4 show the results of optical-model fits to the data with an energy-independent real and imaginary Woods-Saxon potential with parameters $V=100$ MeV, $r_0=1.15$ fm, $a=0.50$ fm, $W=30$ MeV, $r_{i0}=1.28$ fm, and $a_i=0.43$ fm, using the code PTOLEMY [5]. The total reaction cross sections obtained from the

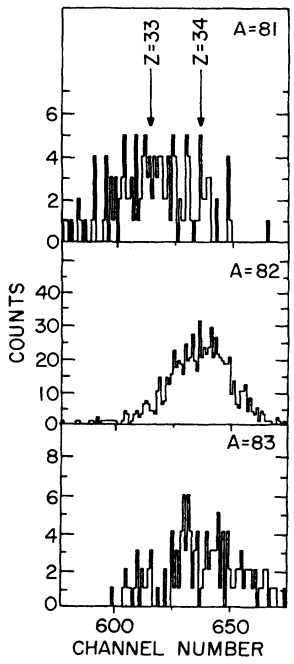

FIG. 3. Measured Z spectra for reaction products with mass 81, 82, and 83 obtained for ^{82}Se+^{198}Pt at $\theta_{lab}=50°$ and $E_{lab}=499.0$ MeV. The arrows indicate the expected position of the $Z=33$ and 34 contributions.

TABLE I. Total reaction cross sections σ_r for ^{76,82}Se+^{192,194,198}Pt obtained from an optical-model (OM) and quarter-point ($\theta_{1/4}$) analysis of elastic plus inelastic scattering.

Projectile	Target	$E_{c.m.}$ (MeV)	σ_r(OM)[a] (mb)	$\sigma_r(\theta_{1/4})$[b] (mb)
^{76}Se	^{192}Pt	349.4	1470	1530
^{76}Se	^{194}Pt	350.4	1550	1510
^{76}Se	^{198}Pt	352.4	1610	1620
^{82}Se	^{192}Pt	349.7	1660	1710
^{82}Se	^{194}Pt	350.7	1740	1760
^{82}Se	^{198}Pt	352.9	1800	1760

[a]Optical-model potential: $V=100$ MeV, $r_0=1.15$ fm, $a=0.50$ fm, $W=30$ MeV, $r_{i0}=1.28$ fm, $a_i=0.43$ fm.
[b]Width parameter $\Delta=14.4\hbar$.

optical-model analysis are tabulated in Table I. This table also lists the total reaction cross sections obtained from the quarter-point angle $\theta_{1/4}$ of the sum of elastic and inelastic scattering, using the generalized Fresnel model developed by Frahn [6] with a width parameter $\Delta=14.4\hbar$. The reaction cross sections calculated using the quarter-point angle are consistent with those obtained from the optical-model analysis.

B. Transfer yields

Figure 5 shows the measured angular distributions of the one- and the two-nucleon pickup and stripping channels with $|Q|\leq 20$ MeV for ^{82}Se+^{198}Pt at $E_{lab}=499.0$ MeV. The solid curves in Fig. 5 are fits to the measured angular distributions with the semiclassical formula of

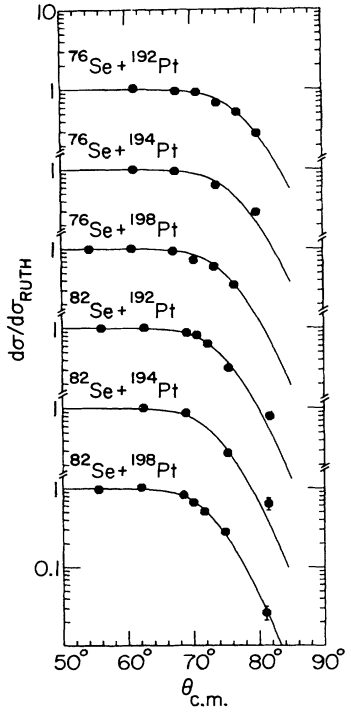

FIG. 4. Elastic-scattering angular distributions for ^{76}Se+^{192,194,198}Pt and ^{82}Se+^{192,194,198}Pt at $E_{lab}=487.7$ and 499.0 MeV, respectively. The solid curves are results of optical-model calculations used to obtain the total reaction cross sections.

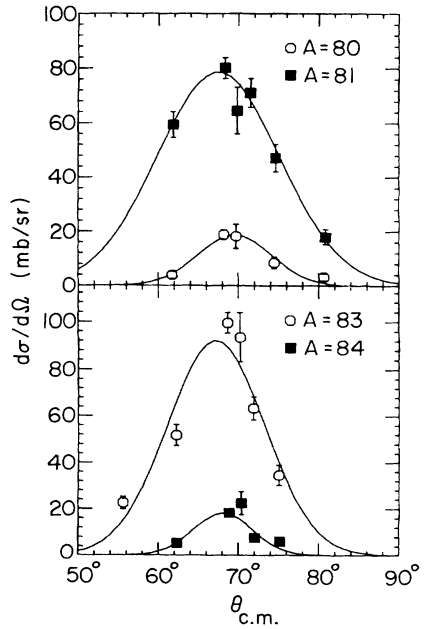

FIG. 5. Measured angular distributions for one- and two-nucleon stripping and pickup reactions for ^{82}Se+^{198}Pt at $E_{lab}=499.0$ MeV. The solid curves shown are fits to the data used to obtain the angle-integrated transfer cross sections.

TABLE II. Measured quasielastic cross sections for one-nucleon pickup (σ_{1Np}), one-nucleon stripping (σ_{1Ns}), two-nucleon pickup (σ_{2Np}), and two-nucleon stripping (σ_{2Ns}) for ^{76,82}Se+^{192,198}Pt.

Beam	Target	$E_{c.m.}$ (MeV)	σ_{1Np} (mb)	σ_{1Ns} (mb)	σ_{2Np} (mb)	σ_{2Np} (mb)
^{76}Se	^{192}Pt	349.4	160±20	85±10	55±20	25±15
^{76}Se	^{198}Pt	352.4	240±40	140±30	50±10	20±15
^{82}Se	^{192}Pt	349.7	95±10	150±25	15±5	40±15
^{82}Se	^{198}Pt	352.9	140±15	150±20	15±5	20±5

Bass [7]. The angle-integrated transfer yields, obtained from these fits, are listed in Tables II and III.

The measurements on ^{194}Pt did not cover enough scattering angles to allow a reliable measurement of the total transfer cross section. The transfer yields discussed in Sec. IV will therefore only include the measurements on the ^{192}Pt and ^{198}Pt targets.

IV. DISCUSSION

A. Total reaction cross sections

The strong absorption radius D can be obtained from the total reaction cross section, deduced from elastic scattering, using the sharp cutoff approximation. The solid squares in Fig. 6 show D as function of $(A_p^{1/3}+A_t^{1/3})$. The solid line shows a fit to the data with $D=r_0(A_p^{1/3}+A_t^{1/3})$, where $r_0=1.44$ fm.

The open circles in Fig. 6 show the distance of closest approach, calculated using Rutherford trajectories, at which the one-neutron pickup cross section peaks as function of $(A_p^{1/3}+A_t^{1/3})$. On average, the transfer probability peaks at a distance 0.6 fm outside the strong absorption radius (the corresponding distance observed for the Ni+Sn system [1] is 1.1 fm).

Figure 7 shows D_{tr} as function of $(A_p^{1/3}+A_t^{1/3})$ for the Se+Pt, Ni+Ni (Ref. [8]), Ni+Sn (Ref. [9]), Ni+Sm (Ref. [2]), Ni+Pb (Ref. [10]), Ni+Th (Ref. [11]), and Si+Ni (Ref. [12]) systems. The solid line shows a fit to the data with $D_{tr}=d_{tr}(A_p^{1/3}+A_t^{1/3})+\Delta d$, where $d_{tr}=1.11$ fm and $\Delta d=4.0$ fm. The trend of the data is very well described by this solid line, indicating that the distance at which the transfer probability peaks is not strongly influenced by the detailed nuclear structure of the projectile and/or target, but depends mainly on the size of the nuclear system.

TABLE III. Measured cross sections for one-neutron and one-proton stripping for ^{76,82}Se+^{192,198}Pt. The error in the one-nucleon stripping yields (σ_{1Ns}) is dominated by the statistical error and the systematic error in the absolute normalization of the data. The errors in the one-neutron and one-proton stripping yields, σ_{1ns} and σ_{1ps}, are mainly due to the poor Z resolution obtained in this measurement.

Projectile	Target	σ_{1Ns} (mb)	σ_{1ns} (mb)	σ_{1ps} (mb)
^{76}Se	^{192}Pt	85±10	30±10	55±15
^{76}Se	^{198}Pt	140±30	25±5	115±30
^{82}Se	^{192}Pt	150±25	65±15	95±25
^{82}Se	^{198}Pt	150±20	65±15	85±20

B. Total quasielastic transfer cross sections

The fraction of the total reaction cross section accounted for by quasielastic transfer for the ^{76}Se- and ^{82}Se-induced reactions is shown as function of the target mass in Fig. 8. The relative strength of quasielastic transfer for the ^{82}Se-induced reactions does not strongly depend on target mass. In contrast, for the ^{76}Se-induced reactions, the relative strength of quasielastic transfer increases from 22% for ^{192}Pt to 28% for ^{198}Pt. This is similar to the results obtained previously for Ni+Sn at comparable energies [1], where the total quasielastic transfer yields again increase strongly with target mass for the ^{58}Ni-induced reactions while they remain fairly constant for the ^{64}Ni-induced reactions.

C. One-nucleon pickup and stripping reactions

The open bars in Figs. 9(a) and 9(b) show the measured angle-integrated cross sections for one-neutron pickup. In order to evaluate the extent to which Q-matching

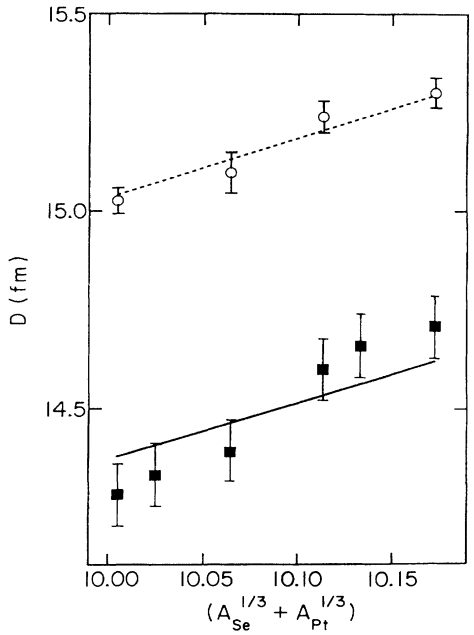

FIG. 6. The strong-absorption radius D (solid squares) and the distance at which the one-neutron pickup cross section peaks (open circles) plotted as function of $(A_p^{1/3}+A_t^{1/3})$. The solid and dashed lines show the results of fits to the data as discussed in the text.

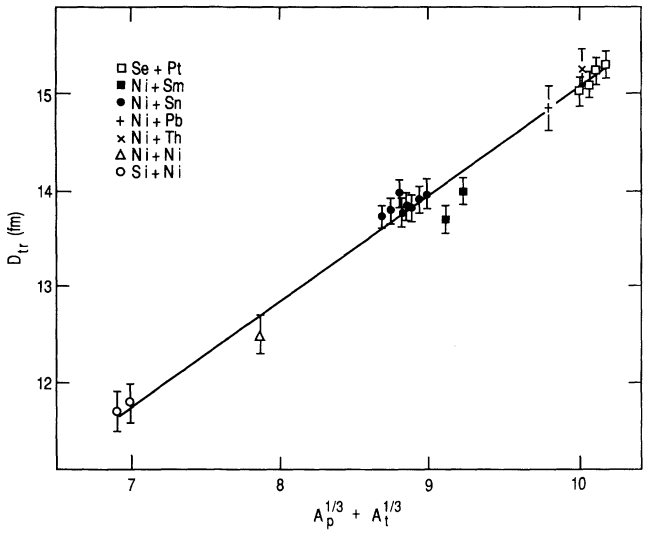

FIG. 7. The distance of closest approach, D_{tr}, at which the transfer cross section peaks, plotted as function of $(A_p^{1/3}+A_t^{1/3})$ for the $^{76,82}Se+^{192,198}Pt$, $^{58}Ni+^{64}Ni$ (Ref. [8]), $^{58,64}Ni+^{112,116,120,124}Sn$ (Ref. [9]), $^{58}Ni+^{144,154}Sm$ (Ref. [2]), $^{58}Ni+^{208}Pb$ (Ref. [10]), $^{58}Ni+^{232}Th$ (Ref. [11]), and $^{28}Si+^{58,62}Ni$ (Ref. [12]) systems. The solid line shows the function $D_{tr}=1.11(A_p^{1/3}+A_t^{1/3})+4.0$.

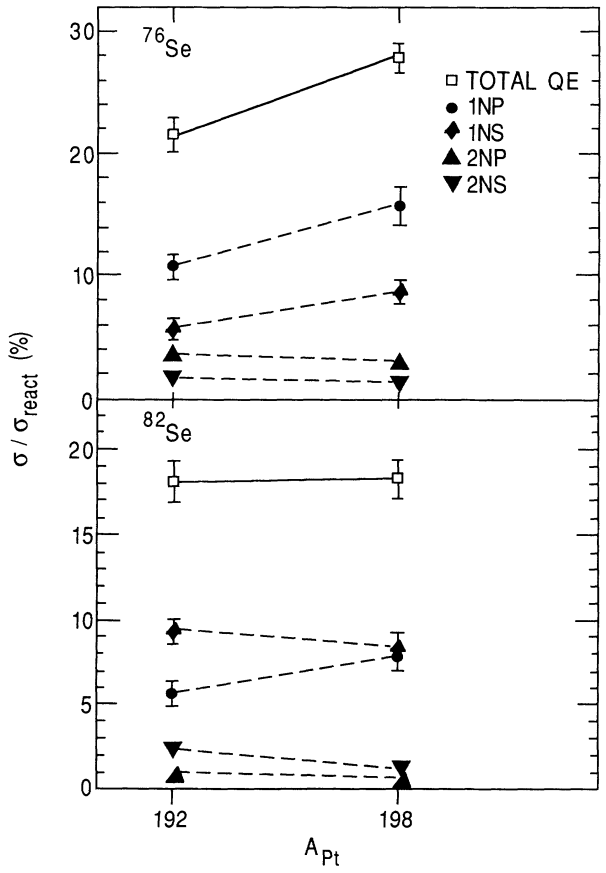

FIG. 8. Strength of the total quasielastic transfer yields, and the one- and two-nucleon pickup/stripping yields shown as fraction of the total reaction cross section vs the target mass for ^{76}Se- and ^{82}Se-induced reactions.

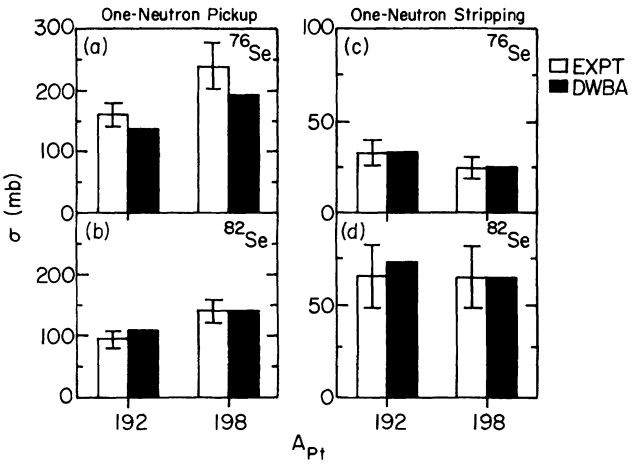

FIG. 9. Cross sections for (a), (b) one-neutron pickup and (c), (d) one-neutron stripping. Shown are the measured yields (open bars), and yields obtained from DWBA calculations (solid bars) normalized to the data for $^{82}Se+^{198}Pt$.

effects influence these transfer processes, we have carried out distorted-wave Born approximation (DWBA) calculations with the code PTOLEMY [5], assuming pickup of a $3p_{3/2}$ neutron in the target, and transferring it to a $2p_{1/2}$ orbit in the projectile. The reaction Q value was taken to be equal to the ground-state Q value. The calculations were done with the bound-state parameters of $r_0=1.2$ fm and $a=0.65$ fm, and the optical potential obtained from fits to the measured elastic-scattering angular distributions. Normalizing the strength of the calculated cross section to the data for $^{82}Se+^{198}Pt$, we obtain the results shown by the solid bars in Figs. 9(a) and 9(b). The variations in the quasielastic cross sections for one-neutron pickup as function of projectile and target mass is quite well reproduced. A comparison between the measured and the calculated angular distribution for $^{82}Se+^{198}Pt$ is shown in Fig. 10. The solid curve shows the results of

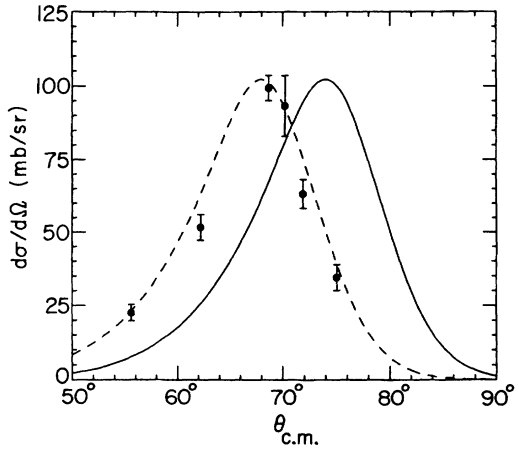

FIG. 10. Measured angular distribution for $^{198}Pt(^{82}Se,^{83}Se)^{197}Pt$ at $E_{lab}=499.0$ MeV. The solid curve shows the result of the DWBA calculations discussed in the text. The dashed curve shows the result of DWBA calculations after an angle shift of $-6°$ has been applied.

the DWBA calculations, with the height normalized to the data. The centroid of the calculated distribution is shifted backwards by 6° with respect to the measured distribution. This shift in angle has been observed in various other heavy-ion reactions [13–17]. Tamura *et al.* [14] have shown that for several systems this shift in angle can be removed by carrying out coupled-channels Born approximation calculations, or by DWBA calculations in which the value of r_0 for the outgoing channel is increased. The dashed curve in Fig. 10 shows the calculated angular distribution, shifted by $-6°$. The DWBA calculation clearly reproduces the width of the measured angular distribution.

DWBA calculations similar to those just discussed for the one-neutron pickup reactions have been carried out for the one-neutron stripping reactions. The DWBA calculations were carried out for the transfer of a $2p_{1/2}$ neutron in the projectile to a $3p_{3/2}$ orbit in the target. The same bound-state parameters and optical potential as for the one-neutron pickup calculations were used. Normalizing the strength of the calculated cross section to the data for ^{82}Se+^{198}Pt, we obtain the results shown in Figs. 9(c) and 9(d). Again, these simple DWBA calculations reproduce the variations of the measured one-neutron stripping yields as function of the mass of the projectile and target quite well.

The dependence of the one-neutron transfer yields at bombarding energies between 10 and 80% above the Coulomb barrier on the ground-state Q value has been studied in detail by van den Berg *et al.* [2]. These authors show that the dependence of the reduced transfer cross section [obtained by multiplying the measured yield by $(B_iB_f)^{1.1}$, where B_i and B_f are the ground-state binding energies of the transferred neutron in the entrance and exit channels, respectively] on the ground-state Q value can be understood on the basis of Q-matching behavior [2]. The solid data points in Fig. 11 show the reduced cross sections for one-neutron transfer for ^{76,82}Se+^{192,198}Pt as function of the ground-state Q value. The open data points show the reduced yields for one-neutron transfer in several other heavy-ion reactions induced by projectiles with mass between $A=28$ and 64, on targets ranging from ^{58}Ni to ^{208}Pb. The solid curve in Fig. 11 shows the result of a least-squares fit to the data discussed by van den Berg *et al.* [2]. Clearly, the one-neutron transfer data obtained for ^{76,82}Se+^{192,198}Pt are in good agreement with the observed systematic for other heavy-ion interactions.

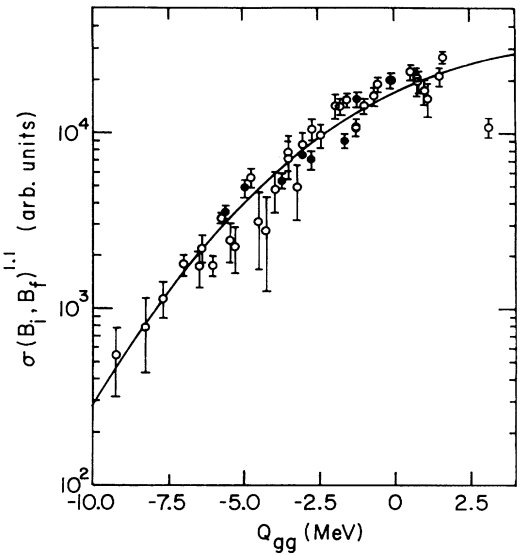

FIG. 11. Reduced cross section for one-neutron transfer as function of the ground-state Q value. The solid data points show the measured yields for ^{76,82}Se+^{192,198}Pt. The open data points show the measured one-neutron transfer cross sections for several other heavy-ion systems. The solid curve is a fit to the data discussed in Ref. [2].

D. Two-nucleon pickup and stripping reactions

The yields for two-nucleon transfer are small, and account for, at most, 6% of the total reaction cross section. These yields are larger than one would expect if two-nucleon transfer would be the result of two consecutive single-nucleon transfer reactions. The ratio of the measured yield for two-nucleon transfer and the yield expected for two consecutive single-nucleon transfer reactions, calculated as in Ref [17], is between 3 and 5 for ^{76,82}Se+^{192}Pt, and between 1.4 and 1.7 for ^{76,82}Se+^{198}Pt. This enhancement of the two-nucleon transfer cross section has been observed in many other heavy-ion systems and is thought to be a result of nucleon pairing [9,10,17–20]. The usual interpretation of the transfer data in terms of a transfer probability as function of the distance of closest approach cannot be applied to our data since most of the data points were measured at angles beyond the grazing angle, corresponding to distances of closest approach within the strong absorption radius. In the region where the transfer probability should show an exponential dependence on the distance of closest approach, only one or two data points have been measured.

V. SUMMARY

Cross sections for elastic scattering and quasielastic transfer have been measured for ^{76,82}Se+^{192,194,198}Pt at bombarding energies about 35% above the Coulomb barrier. The quasielastic cross sections increase with increasing target mass for the ^{76}Se-induced reactions, while they are constant for the ^{82}Se-induced reactions. This is similar to what has been observed in the Ni+Sn system [1,9]. The total quasielastic yields are dominated by one-nucleon transfer. The one-nucleon pickup yields are dominated by one-neutron pickup, while the one-nucleon stripping yields contain significant contributions from both one-neutron and one-proton stripping. The variation of the one-neutron transfer yields as function of projectile and target mass can be understood on the basis of Q matching. The strength of two-nucleon transfer varies between 13 and 32% of that of one-nucleon transfer. Quasielastic transfer accounts for, at most, 30% of the total reaction cross section. For a heavy system, like Se+Pt, it is expected that fusion is a weak reaction channel, and that the remaining strength is probably due to deep-inelastic scattering.

ACKNOWLEDGMENTS

We express our gratitude to the accelerator crew of ATLAS for providing us with ^{76}Se and ^{82}Se beams of excellent quality. This work was supported in part by the U.S. Department of Energy, Nuclear Physics Division, under Contract No. W-31-109-ENG-38 and in part by the National Science Foundation.

[1] A. M. van den Berg, W. Henning, L. L. Lee, K. T. Lesko, K. E. Rehm, J. P. Schiffer, G. S. F. Stephans, F. L. H. Wolfs, and W. S. Freeman, Phys. Rev. Lett. **56**, 572 (1986).

[2] A. M. van den Berg, K. E. Rehm, D. G. Kovar, W. Kutschera, and G. S. F. Stephans, Phys. Lett. B **194**, 334 (1987).

[3] J. R. Erskine, T. H. Braid, and J. G. Stoltzfus, Nucl. Instum. Methods **135**, 67 (1976).

[4] R. Pardo, B. E. Clifft, P. Denhartog, D. Kovar, W. Kutschera, and K. E. Rehm, Nucl. Instrum. Methods A **270**, 226 (1988).

[5] S. C. Pieper, M. H. Macfarlane, and M. Rhoades-Brown, Argonne National Laboratory Report No. ANL-76-11, 1976 (unpublished).

[6] W. E. Frahn, Nucl. Phys. **A302**, 267 (1978).

[7] R. Bass, *Nuclear Reactions with Heavy Ions* (Springer-Verlag, Berlin, 1980), p. 143, Eq. (4.21).

[8] K. E. Rehm, F. L. H. Wolfs, A. M. van den Berg, and W. Henning, Phys. Rev. Lett. **55**, 280 (1985).

[9] A. M. van den Berg, W. Henning, L. L. Lee, K. T. Lesko, K. E. Rehm, J. P. Schiffer, G. S. F. Stephans, F. L. H. Wolfs, and W. S. Freeman, Phys. Rev. C **36**, 178 (1988).

[10] K. E. Rehm, D. G. Kovar, W. Kutschera, M. Paul, G. S. F. Stephans, and J. L. Yntema, Phys. Rev. Lett. **51**, 1426 (1983).

[11] K. E. Rehm, F. L. H. Wolfs, W. Kutschera, and A. Wuosmaa, to be submitted to Phys. Rev. C.

[12] Y. Sugiyama, Y. Tomita, H. Ikezoe, K. Ideno, N. Shikazono, N. Kato, H. Fujita, T. Sugimitsu, and S. Kubono, Phys. Lett. B **302**, 302 (1986).

[13] W. von Oertzen, H. Homeyer, B. G. Harvey, D. Hendrie, and D. Kovar, Z. Phys. A **279**, 357 (1976).

[14] T. Tamura, T. Udagawa, and M. C. Mermaz, Phys. Rep. **65**, 345 (1980).

[15] S. D. Hoath, G. C. Morrison, J. M. Nelson, P. Videbaek, P. D. Bond, Ole Hansen, M. J. Levine, C. E. Thorn, and W. Trautmann, Phys. Lett. **154B**, 33 (1985).

[16] M. F. Vineyard, D. G. Kovar, G. S. F. Stephans, K. E. Rehm, G. Rosner, H. Ikezoe, J. J. Kolata, and R. Vojtech, Phys. Rev. C **33**, 1325 (1986).

[17] W. von Oertzen, H. G. Bohlen, B. Gebauer, R. Künkel, F. Pühlhofer, and D. Schüll, Z. Phys. A **326**, 463 (1987).

[18] I. Chiodi, S. Lunardi, M. Morando, C. Signorini, G. Fortuna, W. Starzecki, A. M. Stefanini, G. Korschinek, H. Morinaga, E. Nolte, and W. Schollmeier, Nuovo Cimento **33**, 159 (1982).

[19] R. Künkel, W. von Oertzen, H. G. Bohlen, B. Gebauer, H. A. Bösser, B. Kohlmeyer, F. Pühlhofer, J. Speer, and D. Schüll, Phys. Lett. B **208**, 355 (1987).

[20] R. Künkel, W. von Oertzen, H. G. Bohlen, B. Gebauer, H. A. Bösser, B. Kohlmeyer, F. Pühlhofer, J. Speer, and D. Schüll, Z. Phys. A **336**, 71 (1990).